Noninvasive Imaging: Brillouin Confocal Microscopy

16

Miloš Nikolić, Christina Conrad, Jitao Zhang, and Giuliano Scarcelli

Abstract

In the past decades, there has been increased awareness that mechanical properties of tissues and cells are closely associated with disease physiology and pathology. Recognizing this importance, Brillouin spectroscopy instrumentation, already utilized in physics and material science, has been adopted for cell and tissue biomechanics. For biomedical applications, progress of Brillouin spectrometer technology has been crucial, mainly improvement in the acquisition speed and combination with confocal microscopy, to enable measurement of material longitudinal modulus in three dimensions with high spatial resolution. Micron spatial resolution and high sensitivity allow mapping intracellular modulus and distinguishing between nuclear and cytoplasmic mechanical properties as well as detecting changes due to perturbations of individual cellular components. In cancer, environmental mechanical factors and intracellular mechanics are expected to play an integral role in cancer progression and treatment success. Brillouin confocal microscopy is appealing for many studies in cancer mechanobiology involving both primary tumors and metastatic dissemination. Specifically, Brillouin technology is suitable for experimental scenarios where noncontact mechanical measurements are required such as 3D tumor models, interactions with the extracellular matrix (ECM), investigation of nuclear mechanical properties, or analysis of cells within microfluidic chips.

M. Nikolić (✉)
Maryland Biophysics Program, University of Maryland, College Park, MD, USA
e-mail: mnikolic@umd.edu

C. Conrad · J. Zhang (✉)
Fischell Department of Bioengineering, University of Maryland, College Park, MD, USA
e-mail: cconrad8@umd.edu; jtzhang4@umd.edu

G. Scarcelli (✉)
Maryland Biophysics Program, University of Maryland, College Park, MD, USA

Fischell Department of Bioengineering, University of Maryland, College Park, MD, USA
e-mail: scarc@umd.edu

Keywords

Light scattering · Brillouin scattering · Confocal microscopy · Elastic modulus · 3D imaging · Biomechanics · Local mechanical properties · Noncontact technique · Noninvasive measurement

C. Dong et al. (eds.), *Biomechanics in Oncology*, Advances in Experimental Medicine and Biology 1092, https://doi.org/10.1007/978-3-319-95294-9_16

16.1 Introduction

For nearly a century, Brillouin scattering has been used to characterize mechanical properties of materials. In the last decade, there has been increased awareness that mechanical properties of tissues and cells are closely associated to disease physiology and pathology. Recognizing this importance, Brillouin spectroscopy instrumentation has been adopted for cell and tissue biomechanics. Specifically, the progress in acquisition speed of Brillouin spectrometers has enabled combining the spectroscopy technique with confocal microscopy to provide maps of material longitudinal modulus at high three-dimensional (3D) spatial resolution. Current spatial resolution allows mapping intracellular modulus, thus distinguishing nuclear modulus from cytoplasmic modulus without contact and with enough sensitivity to detect changes due to perturbations of individual cellular components.

Brillouin microscopy could greatly advance some of the open questions regarding the mechanical behaviors of cells and their microenvironment throughout cancer progression timeline; from primary tumor growth, throughout the metastatic cascade, and secondary tumor development. Environmental mechanical factors and intracellular mechanics are expected to play an integral role in metastatic progression as well as in the development of therapy resistance. To characterize the behavior of cells, numerous groups are working to develop tumor models using three-dimensional cell culture techniques and microfluidic chips. Brillouin spectroscopy can work hand in hand with these tools for characterizing the mechanical properties during tumor development in experimental settings where cells cannot be contacted, and thus previous mechanical characterization techniques cannot be used.

16.2 Measuring Cell Biomechanics

Live cells sense mechanical cues from the environment and activate biochemical pathways in response to them. Furthermore, they remodel their environment, thus giving rise to a series of complex mechanical interaction processes. These mechanical interactions critically determine the cell behavior and many cellular functions, such as proliferation, migration, and gene expression [1, 2], as well as system-level behaviors, such as tissue morphogenesis, angiogenesis, and metastasis [3–5]. For this reason, the past two decades have witnessed a large interest toward designing technologies that can detect the mechanical properties of biological processes on the cellular level.

The most widely used techniques for cellular elasticity measurements include atomic force microscopy (AFM) [6], micropipette aspiration (MP) [7], magnetic twisting cytometry (MTC) [8], optical stretchers (OS) [9], microfluidic deformability cytometry (MDC) [10, 11], and microrheology [12]. These methods have enabled tremendous progress in cell mechanic studies over a large range of spatial and temporal scales. AFM and AFM-based microindentation apply precise known forces on a cell through a cantilever and give a deformation value to extract cell modulus. AFM can achieve nm-spatial resolution but suffers from poor temporal resolution (up to hours). Micropipette aspiration precisely tracks a cell as it is aspirated into a small glass tube under controlled suction pressure to back-calculate the cell's resistance to deformation. Micropipette aspiration enables accurate readings of the viscoelastic response with single cell resolution. MTC uses magnetic beads functionalized to bind to the surface of a cell and monitors the resistance of the bead-cell complex being twisted under a magnetic field. As a result, MTC is best suited to characterize subcellular components such as the cortex. OS use two counter-propagating laser beams co-focused on the same cell to generate a stretching force while monitoring cell deformation through light microscopy. Similarly, MDC used fluidic forces to generate a stretching force on a cell while monitoring cell deformation with a high-speed camera. Both OS and MDC do not provide a direct readout of the cell modulus as they measure deformations but have dramatically enhanced our ability to measure cell mechanics at

high throughput. Microrheology is an example of a non-contact technique. By injecting fluorescent tracers into the cell, and measuring the thermal motion of the tracers, the local elasticity can be inferred. Being contact-free may be an important advantage of microrheology, given that cells are able to remodel and respond to mechanical stresses. On the other hand, the technique assumes that the tracer motion is Brownian; moreover, in practice it is not easy to track many tracers simultaneously thus providing a patchwork of measurements rather than the full map of cell mechanical properties. Other non-perturbative methods to measure material mechanics such as acoustic microscopy, ultrasound, or optical elastography [13, 14] are limited to tissue mechanics studies as their spatial resolution is not sufficient for cell studies.

These techniques have enabled immense progress of cell biomechanics in the past few decades. For instance, they have facilitated experiments that probed how mechanical properties of cells and their environment can lead to malignant transformation. Elastic signatures on the cellular and subcellular level have been shown to be good markers for cell diagnosis such as malignancy. AFM studies were the first to show that live metastatic cells from patients are significantly softer than normal cells [15]. These findings have been confirmed with other techniques [16, 17], including recently with deformability cytometry [18].

However, most of these studies have been limited to cells grown on flat substrates or in suspension since cells must be contacted for the measurement. Brillouin microscopy is an addition to this toolbox that can extend cell biomechanical studies to experimental settings where cells cannot be easily accessed. For example, experiments can be easily performed within microfluidic chips, or in 3D cultures. Also, potential measurements can be done in vivo within tissue due to the ability of Brillouin microscopy to directly measure cell longitudinal modulus, with spatial resolution of a standard confocal microscope without contact or perturbation of the biological sample under study.

16.3 Brillouin Scattering

Brillouin scattering is named after Léon Brillouin, who published the theory that predicted this phenomenon in 1922 [19]. At nearly the same time, Leonid Mandelstam also studied the behavior of interactions between photons and phonons, and he published his findings in 1926. This type of interaction is sometimes referred to as Brillouin-Mandelstam scattering.

Brillouin scattering is the inelastic scattering of light from thermal phonons, or thermally generated density/pressure waves (Fig. 16.1a). The scattering is said to be inelastic, because there is a change in frequency (or color) of the scattered light. This frequency shift is proportional to the energy of the thermally generated sound wave. The theory of Brillouin scattering emerged in the early twentieth century, after the advances in theory of waves, such as those by Doppler and Bragg. In 1842 Doppler described the frequency shift of waves with moving sources; in 1913 Bragg worked out the conditions for scattering of light from periodic crystalline structures. In fact, one can most easily describe Brillouin scattering as the scattering of light from a periodic structure—a moving sound wave. The Doppler shift in frequency is produced because the sound waves are traveling inside the scattering medium. In this way Brillouin scattering provides information about the thermal density fluctuations in the scattering sample and opens an avenue for direct measurement of related physical properties in materials.

For a quantitative derivation, consider the scattering of light of frequency ω from an object. Following the derivation of Ref. [20], denote the incoming wavevector by $\vec{k}_i$ and the wavevector of the scattered light by $\vec{k}_s$. We define q, the wavevector transfer, as

$$\vec{q} = \vec{k}_s - \vec{k}_i$$

The vector $\vec{q}$ points in the direction of the travel of the sound wave (Fig. 16.1b).

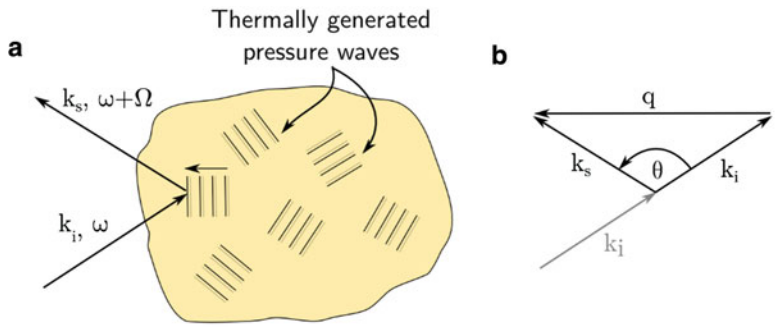

Fig. 16.1 (**a**) Diagram of the light scattering from thermal phonons inside a material. (**b**) Vector diagram of the scattering process

Thermal phonons travel with the speed of sound v_s that is related to the local mechanical properties of the material

$$v_s = \sqrt{\frac{M}{\rho}}$$

where M is the longitudinal elastic modulus of the material, and ρ is the mass density.

The wavevector $\vec{q}$ and the frequency of the thermal pressure waves are related by the linear dispersion relation

$$\Omega = \sqrt{\frac{M}{\rho}}\, q$$

It can be shown that the scattered light will experience an upward and downward frequency shift from the frequency of the incident light ω_i. The frequency of the scattered light ω_s is given by

$$\omega_s = \omega_i \pm \Omega$$

Since the frequency shift is very small (10^{-5}–10^{-6} times smaller than the frequency of the laser light), the lengths of the incident and scattered wavevectors are approximately the same. The intensity of the wavevector transfer q can be written as

$$q = 2nk \sin\left(\frac{\theta}{2}\right) = \frac{4\pi n}{\lambda} \sin\left(\frac{\theta}{2}\right)$$

Then, the Brillouin shift can be written as a function of the longitudinal modulus, mass density, index of refraction, and the known parameters of the scattering experiment.

$$\Omega = \sqrt{\frac{M}{\rho}}\ \frac{4\pi n}{\lambda} \sin\left(\frac{\theta}{2}\right)$$

Since the index of refraction in cells directly correlates with the mass content (ρ), the factor $n/\sqrt{\rho}$ can be considered a constant inside cells. Based on published data, the value of $\frac{\rho}{n^2}$ is estimated to vary at most a few percent within cells and tissue [21, 22]. This allows to approximate the index/density factor as constant. Thus, the relative longitudinal modulus has one-to-one mapping to Brillouin frequency shift measured directly by spectroscopy $\Omega \propto \sqrt{M}$.

16.3.1 Longitudinal Modulus

Brillouin frequency shift provides a measurement of the local longitudinal modulus within the probed volume inside the sample. In a solid material, longitudinal modulus is the ratio of the uniaxial stress to the uniaxial strain, and can be related to Young's shear modulus and bulk modulus, in a straightforward manner [23].

Figure 16.2 illustrates the geometry of stress and strain of an object in several cases that can each be quantified by various elastic moduli. In elastic solids, the relationship between longitudinal modulus and other mechanical moduli is well known. The longitudinal modulus is similar to the Young's modulus as they both describe a uniaxial stress-strain test, but the key difference is that in the case of Young's modulus, the object is also

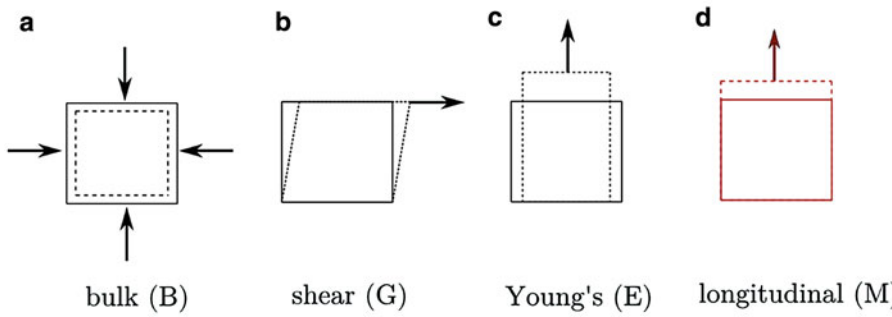

Fig. 16.2 Illustration of stress-strain relationships that are described by (**a**) bulk, (**b**) shear, (**c**) Young's, and (**d**) longitudinal moduli. Bulk elastic modulus describes the amount of volume change of an object due to a change in the pressure. Shear and Young's moduli are the most commonly measured in lab using conventional rheometers, since they describe the geometric deformation of an object when a constant stress is applied in a fixed direction. Longitudinal modulus quantifies the relationship between the uniaxial stress and the uniaxial strain

allowed to deform in the direction perpendicular to the applied stress.

In general, to completely describe the elastic properties of a material, one must consider the complete elastic tensor c_{ijkl} [23]. For a general material, this is a fourth-rank tensor, with 21 independent elements that relate the stress to strain. For example, the elastic tensor of an isotropic material is given below. This tensor can be simplified due to symmetry, and it can be expressed using only two independent parameters. It is given by the following 6×6 reduced notation[1] matrix.

c_{11}	c_{12}	c_{12}	0	0	0
	c_{11}	c_{12}	0	0	0
		c_{11}	0	0	0
			$\frac{1}{2}(c_{11}-c_{12})$	0	0
				$\frac{1}{2}(c_{11}-c_{12})$	0
					$\frac{1}{2}(c_{11}-c_{12})$

The element c_{11} is the longitudinal modulus M, while c_{12} is known as the Lamé constant λ. The element $\frac{1}{2}(c_{11}-c_{12})$ is the shear modulus G. Young's modulus is

$$\frac{(c_{11}-c_{12})(c_{11}+2c_{12})}{c_{11}+c_{12}}.$$

In terms of bulk modulus B and shear modulus G, the complete elastic tensor for an isotropic material can be written as.

$B+\frac{4}{3}G$	$B-\frac{2}{3}G$	$B-\frac{2}{3}G$	0	0	0
	$B+\frac{4}{3}G$	$B-\frac{2}{3}G$	0	0	0
		$B+\frac{4}{3}G$	0	0	0
			G	0	0
				G	0
					G

In theory for crystalline materials, Brillouin shift gives us the ability to directly measure the full elastic tensor. This intriguing possibility has been recently demonstrated in silk and collagen by varying the scattering angle [24, 25]. However, biological tissue and cells do not follow the straightforward rules of elastic solids. In these the relationship between longitudinal modulus and other moduli is more complex. First, for the application of measuring cells and tissue, due to their near incompressibility and high water content, the shear modulus is significantly smaller than the bulk modulus ($G << B$). Therefore, the longitudinal modulus measured by Brillouin spectroscopy is much higher than the traditional Young's or shear moduli. Second, in biological materials, the value of the elastic constants usu-

[1]Each numerical index denotes one of the following pairs of Cartesian indices. $1 = xx$, $2 = yy$, $3 = zz$, $4 = yz = zy$, $5 = xz = zx$, $6 = xy = yx$.

ally depends on the timescale on which the force is applied. Namely, the elastic tensor depends on the frequency of the periodically applied stress. In practice, two limiting regimes are usually considered: the low frequency $c_{ij}(0)$ and high frequency $c_{ij}(\infty)$. The regular mechanical rheometers perform quasi-static measurements, and they measure $c_{ij}(0)$ while techniques such as Brillouin scattering measure the $c_{ij}(\infty)$, the elastic tensor at high frequency. In liquids and polymers, the high-frequency component of the elastic tensor has a higher value, because during fast deformation of the material, some of the slower molecular relaxation processes do not have any contribution, thus effectively "stiffening" up the material. It has been shown that there exists a strong correlation between the mechanically measured low-frequency elasticity (shear or Young's moduli) and high-frequency Brillouin elasticity (longitudinal modulus).

$$\log M = a \ \log G + b.$$

where G is the shear (or Young's) modulus measured at low frequency and a and b are material-dependent coefficients [21, 22]. This empirical correlation is consistent with the power-law scaling of elastic moduli with frequency that has previously been found in tissue, polymers, and cytoskeleton [26, 27]. However, the interpretation of the longitudinal modulus in the cell-matrix context and its relation to traditional quasi-static Young's modulus still need thorough theoretical understanding.

16.3.2 Brillouin Instrumentation

For many decades, the spectra of Brillouin scattered light have been used to characterize the mechanical properties of materials such as glass, polymers, metals, and minerals [28]. In common materials and in backscattering configuration, the frequency shift of Brillouin scattered light is on the order of 5–10 GHz. A 5 GHz frequency shift of the 532 nm laser corresponds to about 0.005 nm change in the wavelength. This is a very small change that cannot be measured with traditional filters or grating-based spectrometers used in Raman or Fluorescence measurements. The basis of spectrometer design for many years has been a Fabry-Perot interferometer where high spectral resolution is obtained through the multiple interference of light at two parallel reflecting surfaces. Specifically, in the 1970s, Sandercock demonstrated the use of a multi-pass Fabry-Perot interferometer to achieve accurate measurements of Brillouin scattering in a reliable instrument [29]. Instruments based on Sandercock's design have been the workhorse of Brillouin spectroscopy research throughout the world for nearly 50 years. In the 1980s, the first biological characterization was performed by Vaughan and Randall, who characterized elastic properties of the lens and cornea of the eye [30, 31]. However, Brillouin research in biology has been scarce since then because the multi-pass FP interferometer has very long acquisition times (minutes to hours per single spectrum).

This bottleneck was overcome in 2008 when Brillouin spectrometers based on a different element, the virtually imaged phase array (VIPA), were introduced by Scarcelli and Yun which overcame the speed limitations of traditional Fabry-Perot interferometers [32]. VIPA etalons had been first developed in 1996 by Shirasaki [33]; similarly to FP interferometers, the high spectral resolution comes from the multiple interference at two parallel reflecting surfaces; unlike FP interferometers though, the front surface is totally reflective (other than for an input anti-reflective window) so that no reflection interference is formed, and all the light is used to form a transmitted pattern. To further improve acquisition speed, VIPA etalons were used in tilted configuration with input divergent beam so that all the different components of the spectra could be measured with one shot. This improvement and the many others on the same VIPA-based platform has led to spectral measurements performed in about 0.1 s which enabled Brillouin-based imaging biological materials [34, 35].

16.3.3 Brillouin Microscopy

Inverted confocal microscope is one possible experimental setup for Brillouin measurement (Fig. 16.3). On most microscopes a port for coupling laser light into the objective is already built in. Lasers of any visible wavelength can be used. For example, 532 nm frequency doubled Nd-YAG is a common choice due to its stability and narrow natural linewidth. Laser light is focused onto the sample by an objective that also serves as the collector lens for the backscattered laser light. In this case the scattering angle θ is 180°, and the Brillouin frequency shift in Hertz can be written as

$$\nu_B = \frac{\Omega}{2\pi} = \frac{2n}{\lambda\sqrt{\rho}}\sqrt{M}.$$

The backscattered light can be separated from the illumination light by using a polarizing beam splitter and a quarter-waveplate, as it is usually done in the confocal reflectance experiments. The collected light is then coupled into a single-mode optical fiber that leads into the Brillouin spectrometer. There is no need for the pinhole in the setup, since the aperture of the optical fiber serves the same purpose and assures that the collected light comes from a single confocal volume in the sample. Thus, the samples can be characterized with a spatial resolution dictated by the objective lens of the confocal microscope.

Current VIPA-based spectrometers are comprised of two apodized cross-axis VIPA stages with a relay telescope and square-hole spatial filter between them [35, 36]. Linearly variable intensity filters are used for apodization [22]. The diffraction pattern after the final VIPA stage is detected with an electron-multiplying charge-coupled device (EM-CCD) camera with low noise, so that very low signals can be detected [37].

To scan the sample in 3D, a motorized stage is placed on the microscope, and laser beam is raster-scanned through the sample space. Brillouin image scans can then be easily acquired, by recording individual spectra for each position in the sample and performing a least squares curve fitting on the spectrum to determine the position of the Brillouin peaks. An example of a 3D scan of a cell sitting on glass is shown in Fig. 16.4. Performing cell measurements is also possible without a motorized stage and within a microfluidic chip by flowing cells and recording the Brillouin shift value as they travel through the focus of the illumination [38].

To become a widely adopted technique in cell and tissue biomechanics, Brillouin technology still needs improvement. Acquisition speed is now at the point that a two-dimensional (2D) image of a single cell with 1 micron resolution takes approximately 2 min. The more recent addition of flow cytometry has enabled cell characterizations at higher throughput [38]. Improving Brillouin microscopy technology is a very active area of research. Specifically, enhancing measurement through nontransparent tissue [39–42], reducing artifacts due to interfaces [43–45], improving acquisition speed [46–48], and integrating program automation for high-throughput sampling have recently seen great progress.

16.4 Intracellular Mechanics

Brillouin microscopy has shown the ability to characterize not only biological tissue [49–54] but also to measure the mechanical properties of cells and subcellular components. In the past few years, several groups have shown the capability of Brillouin microscopy to measure cytoplasmic/cytoskeletal properties and their perturbations. In the cytoplasm, a complex mixture of liquid and solid components regulates cell mechanical properties [55]. The cytoskeleton and its constituent components (actin, microtubules, and intermediate filaments) form the backbone of cell mechanical strength. Focusing on reconstituted actin gels, Scarcelli et al. demonstrated that Brillouin microscopy can detect differences in actin polymerization and branching, two key mechanisms cells used to modulate their internal stiffness [22]. Inside cells, they also observed significant decrease in modulus when perturbing cells with *cytochalasin D*. The molecules of *cytochalasin D* bind strongly to the (+) ends of the

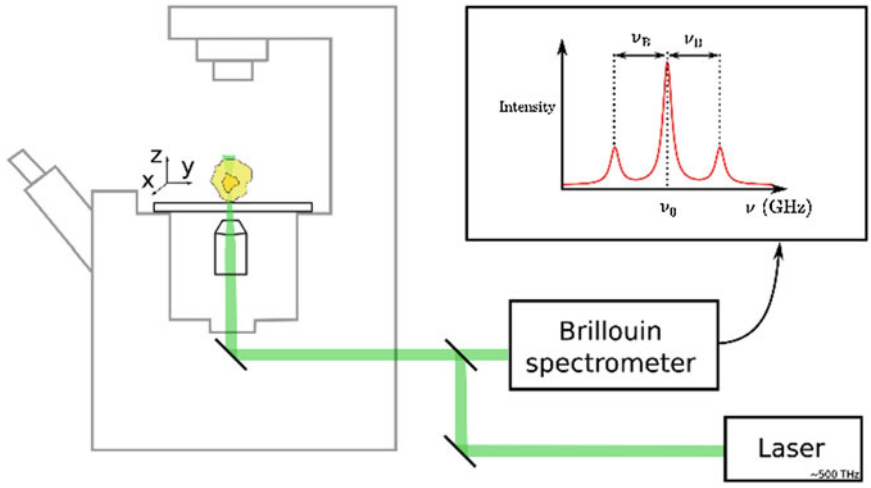

Fig. 16.3 Schematic of the experimental setup. Backscattered laser light is sent to the VIPA-based Brillouin spectrometer which acquires an image of the spectrum on the EMCCD camera. The distance of the Brillouin peaks in GHz from the central laser frequency is a measurement of the local mechanical properties at the confocal volume on the microscope

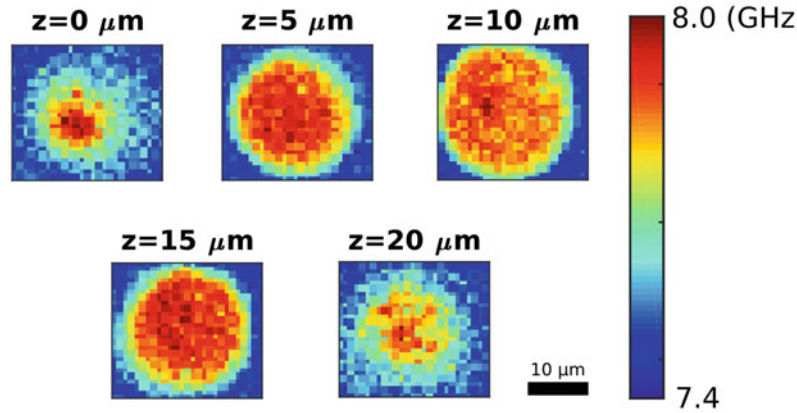

Fig. 16.4 An example of the 3D confocal scan of a detached MCF10A cell that is resting on a glass coverslip. Color represents the measured Brillouin shift in GHz

F-actin, thus preventing new addition of G-actin and the growth of the actin cytoskeleton, which inhibits actin polymerization and thus decreases the stiffness of the cell. Antonacci et al. observed similar effects of reduced modulus using *Latrunculin A*, which is another widely used drug that prevents cytoskeletal assembly [56]. Using plant cells, Elsayad et al. observed that cells do not have uniform modulus, but it is symmetrically patterned when cells undergo directional growth [57]. Using red blood cells, Meng et al. also observed a nonuniform distribution of modulus within the cell featuring the cell edge with higher Brillouin shift than the cell center [58].

Recently, beyond the cytoplasm, Brillouin microscopy was applied to the measurement of nuclear mechanical properties. This is very important as the nucleus is inaccessible from the exterior, and thus nearly all previous mechanical techniques require extraction of the nucleus before characterization. Zhang et al. treated cells with Trichostatin A (TSA), a drug that inhibits the activity of histone deacetylases. This treatment leads to chromatin decondensation, and its effects on cytoplasmic and nuclear stiffness were

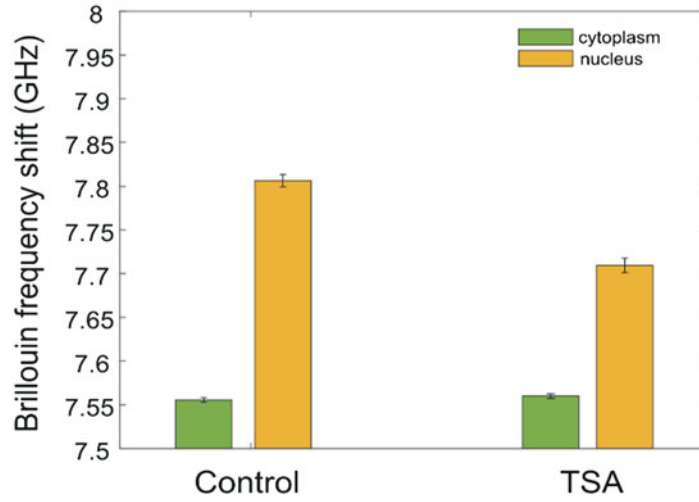

Fig. 16.5 Brillouin Frequency shift of nucleus of NIH 3T3 cells shows significant reduction following TSA treatment

examined by Brillouin microscopy. As shown in Fig. 16.5, the Brillouin frequency shift of TSA-treated cells compared to the control group displayed significant differences. The nucleus presented decreased modulus, while the cytoplasm was not affected by the effects of TSA [38].

All these experiments show that Brillouin microscopy is a powerful addition to the set of techniques for measuring cell mechanics. As a non-contact method, it can be easily used to detect changes inside of the cells that might be difficult to quantify by other means.

16.5 Applications in Cancer Mechanobiology

Biomechanics influences the progression of individual cancer cells in the process of tumorigenesis as well as through cell and tumor interactions with the microenvironment [59]. More recent studies have propelled interest in the intersection between mechanics, genetics, and biochemical pathways associated with cancer progression [60]. As an all optical noncontact technology with micron-scale resolution, Brillouin confocal microscopy is appealing for many studies in cancer mechanobiology involving primary tumors, metastatic dissemination, and interactions with the extracellular matrix (ECM).

16.5.1 Tumor and the Microenvironment

The biomechanical interaction between tumors and the extracellular matrix has been largely established as a critical regulator of tumor progression [61]. Tumor progression is promoted by the extracellular matrix stiffness by enhancement in integrin signaling through a well-known mechanically coupled pathway [5]. Extracellular matrix stiffening has been shown to modulate ERK and Rho pathways, increase cytoskeletal tension, increase integrin expression, and drive the assembly of focal adhesions [59]. On the other hand, the inhibition of integrin signaling through matrix softening lowers the potential for malignancy transformation of mammary epithelial cells [62]. The importance of the mechanical connection between tumors and the extracellular matrix is widely accepted in breast cancer. It has been measured that mammary tumor tissue has a higher elastic modulus than healthy tissue [5, 59, 63]. Diagnostic measures based on these mechanical signatures, such as palpation, ultrasound, and magnetic resonance elastography, are well-established clinical screening procedures [64–66]. However, the link between tumor tissue elastic modulus, genetic signatures, and tumor biochemical pathways is an area which requires further investigation [67]. Moreover, in other

types of cancers, there is limited information regarding tumor stiffness and tumor progression consequences. For example, separate studies analyzing the mechanical properties of glioblastoma tumor tissue showed contrasting view points on the relationship between tumor stiffness and tumor grade [68].

As our understanding of the biochemical and molecular basis of these complex interactions is growing, it is becoming increasingly important to better understand the biomechanical interaction between the tumor and the ECM. Experiments in three-dimensional environments provide an increased number of physiologically relevant parameters; thus, it is crucial to investigate mechanical properties in this manner [69]. Particle-tracking microrheology has been so far the only method to study matrix-cell mechanics in 3D cultures, yet it is suboptimal as it is still invasive and not label-free. Brillouin confocal microscopy enables the characterization of tumor and ECM mechanics without contact at high 3D resolution which can be applied to the characterization of small tumor nodules or cells in 3D microenvironments. This could improve our understanding on the mechanical changes which occur at the cellular level and their correlation with microscopic and macroscopic tissue stiffness.

16.5.2 Mechanical Properties of Metastatic Cells

Biomechanical interactions are thought to be important also in the metastatic cascade. During metastasis cancer cells progress through several phases which include the escape from a primary tumor, intravasation, extravasation, and finally recolonization to a distant location. This series of events involves interaction with many different types of microenvironments, progression through multiple cell types, and modulation through several cell mechanisms (e.g., adhesion, migration, proliferation).

It appears that metastatic cells have an advantage by mechanically softening to facilitate migration and invasion of a crowded ECM environment. Several studies have consistently shown that metastatic cells have a lower elastic modulus compared to non-cancerous ones [15, 70–76]. These studies characterize cells that grow on flat 2D substrates or cells that are floating in suspension. Recent measurements using Brillouin microscopy have shown similar results by comparing the images of non-tumorigenic MCF-10A and metastatic MDA-MB-231 breast epithelial cell lines, as shown in Fig. 16.6.

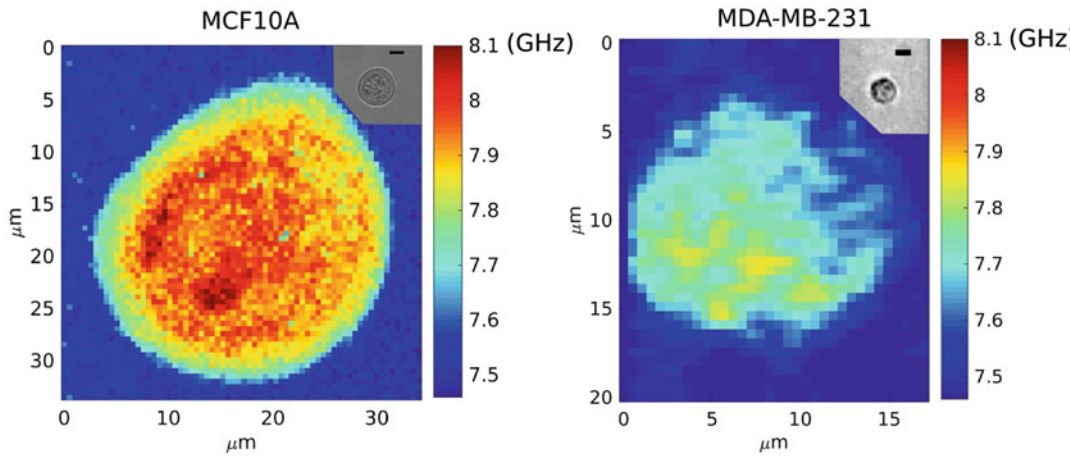

Fig. 16.6 Characterization of the intracellular stiffness of non-tumorigenic MCF-10A and metastatic MDA-MB-231 breast epithelial cell lines. Bright field images are in the insets; scale bar is 10 μm

Mechanical plasticity, i.e., the ability of a cell to change their modulus in response to different mechanical environments, appears to be another advantage for metastatic cells. Malignant cells could possess an increased plasticity compared to normal cell lines which could correlate with increasing metastatic potential [77–79]. The elasticity modulation of cells as a response to the substrate stiffness has been demonstrated in several cell types [80]; Brillouin microscopy has characterized this effect in fibroblasts [51]. The elasticity modulation of metastatic cells in response to different mechanical environments is a central topic to which Brillouin microscopy could contribute much due to the unique ability to investigate cells within different microenvironments.

16.6 Perspectives

The advantage of Brillouin confocal microscopy for studying tumors and metastatic cells is that it can be paired with experiments that put cells in scenarios which mimic real situations that these cells experience or potentially in in vivo settings. Up to now, the elastic moduli of 2D and suspension cell cultures have been measured and have enabled extensive studies of mechanotransduction [15, 70–76]. Brillouin microscopy could extend these types of experiments of cancer mechanobiology in 3D extracellular matrices, during intravasation and extravasation, inside of microfluidic devices, i.e., in experimental settings where direct contact is not possible, and measurements should be non-perturbative. We recently demonstrated this capability in microfluidic channels, which are easily accessible to the Brillouin high-throughput measurement. The mechanical characterization on the population level is potentially very useful for evaluating the heterogeneity in the cancer samples. Furthermore, it is possible to combine Brillouin flow cytometry with other cell-flow techniques such as fluorescence microscopy and cell sorting which opens doors to a wide range of possible experiments. Importantly, Brillouin spectroscopy is a new tool for adding subcellular elastic properties to the list of biomarkers which are accessible to high-throughput flow experiments [38].

In addition, there are a number of robust models that use reconstituted three-dimensional ECM gels to probe the nature of cancer cells [81]. A particular area of interest is the study on in vitro tumors. Despite the advances in the characterization of collective growth of cancer cells, there is still the complex mechanics that takes place during the process of malignant tissue formation [82]. Three-dimensional mechanical properties of both cells and tumors are accessible to the Brillouin microscopy. In the near future, Brillouin studies of the 3D cancer model systems could help shape the understanding of cancer growth in its environment.

Beyond measuring individual cells or tumors, Brillouin microscopy could enable mapping of the mechanical microenvironment. Measurements of the elastic modulus of ECM are critical for mapping the mechanical cues presented to cells, and conversely, for identifying the cell-induced microenvironment modifications [5, 61]. Understanding the bidirectional interaction between cells and their environment is a vigorous area of research, to which Brillouin can contribute precious information about the local mechanical changes occurring because of architectural changes and cell interactions. However, for highly hydrated systems like reconstituted extracellular matrices, current Brillouin signatures need to be further refined [25].

The ultimate application of Brillouin microscopy is to measure in vivo animal models of cancer development. Brillouin microscopy has been previously used in animal and human subjects in vivo for the analysis of ocular tissue [21, 49, 51]. However, being an optical technique with limited signal strength, the penetration depth and the time required to perform a measurement in in vivo setting is currently limited. A strong focus of the instrument development future of Brillouin microscopy thus revolves around the improvement of penetration depth [39–42, 45] and speed of the measurement [46–48]. The translation of Brillouin technology to in

vivo studies could also be accelerated by using multimodal microscopes [22, 57] where faster imaging modalities can characterize large areas of tissue/cells and identify small region of interests or a limited number of points where Brillouin mechanical analysis should be performed.

References

1. Discher DE, Janmey P, Wang YL (2005) Tissue cells feel and respond to the stiffness of their substrate. Science 310:1139–1143
2. Peyton SR, Ghajar CM, Khatiwala CB, Putnam AJ (2007) The emergence of ECM mechanics and cytoskeletal tension as important regulators of cell function. Cell Biochem Biophys 47:300–320
3. Huang S, Ingber DE (2005) Cell tension, matrix mechanics, and cancer development. Cancer Cell 8: 175–176
4. Ingber DE (2002) Mechanical signalling and the cellular response to extracellular matrix in angiogenesis and cardiovascular physiology. Circ Res 91:877–887
5. Levental KR, Yu HM, Kass L, Lakins JN, Egeblad M, Erler JT, Fong SFT, Csiszar K, Giaccia A, Weninger W, Yamauchi M, Gasser DL, Weaver VM (2009) Matrix crosslinking forces tumor progression by enhancing integrin signaling. Cell 139:891–906
6. Kristian F (2011) Atomic force microscopy and its contribution to understanding the development of the nervous system. Curr Opin Genet Dev 21:530–537
7. Evans E, Yeung A (1989) Apparent viscosity and cortical tension of blood granulocytes determined by micropipet aspiration. Biophys J 56:151–160
8. Wang N, Ingber D (1995) Probing transmembrane mechanical coupling and cytomechanics using magnetic twisting cytometry. Biochem Cell Biol 73:327–362
9. Guck J, Ananthakrishnan R, Mahmood H, Moon TJ, Cunningham CC, Kas J (2001) The optical stretcher: a novel laser tool to micromanipulate cells. Biophys J 81:767–784
10. Gossett DR, Tse HTK, Lee SA, Ying Y, Lindgren AG, Yang OO, Rao J, Clark AT, Di Carlo D (2012) Hydrodynamic stretching of single cells for large population mechanical phenotyping. Proc Natl Acad Sci U S A 109:7630–7635
11. Otto O, Rosendahl P, Mietke A, Golfier S, Herold C, Klaue D, Girardo S, Pagliara S, Ekpenyong A, Jacobi A, Wobus M, Topfner N, Keyser UF, Mansfeld J, Fischer-Friedrich E, Guck J (2015) Real-time deformability cytometry: on-the-fly cell mechanical phenotyping. Nat Methods 12:199–202
12. Wirtz D (2009) Particle-tracking microrheology of living cells: principles and applications. Annu Rev Biophys 38:301–327
13. Kennedy BF, Wijesinghe P, Sampson DD (2017) The emergence of optical elastography in biomedicine. Nat Photonics 11:215–221
14. Ophir J, Cespedes I, Ponnekanti H, Yazdi Y, Li X (1991) Elastography - a quantitative method for imaging the elasticity of biological tissues. Ultrason Imaging 13:111–134
15. Cross SE, Jin YS, Rao J, Gimzewski JK (2007) Nanomechanical analysis of cells from cancer patients. Nat Nanotechnol 2:780–783
16. Agus DB, Alexander JF, Arap W, Ashili S, Aslan JE, Austin RH, Backman V, Bethel KJ, Bonneau R, Chen WC, Chen-Tanyolac C, Choi NC, Curley SA, Dallas M, Damania D, Davies PCW, Decuzzi P, Dickinson L, Estevez-Salmeron L, Estrella V, Ferrari M, Fischbach C, Foo J, Fraley SI, Frantz C, Fuhrmann A, Gascard P, Gatenby RA, Geng Y, Gerecht S, Gillies RJ, Godin B, Grady WM, Greenfield A, Hemphill C, Hempstead BL, Hielscher A, Hillis WD, Holland EC, Ibrahim-Hashim A, Jacks T, Johnson RH, Joo A, Katz JE, Kelbauskas L, Kesselman C, King MR, Konstantopoulos K, Kraning-Rush CM, Kuhn P, Kung K, Kwee B, Lakins JN, Lambert G, Liao D, Licht JD, Liphardt JT, Liu LY, Lloyd MC, Lyubimova A, Mallick P, Marko J, McCarty OJT, Meldrum DR, Michor F, Mumenthaler SM, Nandakumar V, O'Halloran TV, Oh S, Pasqualini R, Paszek MJ, Philips KG, Poultney CS, Rana K, Reinhart-King CA, Ros R, Semenza GL, Senechal P, Shuler ML, Srinivasan S, Staunton JR, Stypula Y, Subramanian H, Tlsty TD, Tormoen GW, Tseng Y, van Oudenaarden A, Verbridge SS, Wan JC, Weaver VM, Widom J, Will C, Wirtz D, Wojtkowiak J, Wu PH, Phys Sci Oncology Ctr N (2013) A physical sciences network characterization of non-tumorigenic and metastatic cells. Sci Rep 3:1449
17. Remmerbach TW, Wottawah F, Dietrich J, Lincoln B, Wittekind C, Guck J (2009) Oral cancer diagnosis by mechanical phenotyping. Cancer Res 69:1728–1732
18. Tse HTK, Gossett DR, Moon YS, Masaeli M, Sohsman M, Ying Y, Mislick K, Adams RP, Rao JY, Di Carlo D (2013) Quantitative diagnosis of malignant pleural effusions by single-cell mechanophenotyping. Sci Transl Med 5:212ra163
19. Brillouin L (1922) Diffusion de la lumiere et des rayonnes X par un corps transparent homogene influence del'agitation thermique. Ann Phys 17:88–122
20. Boyd R (1992) Nonlinear optics. Academic Press, London
21. Scarcelli G, Kim P, Yun S (2011) In vivo measurement of age-related stiffening in the crystalline lens by Brillouin optical microscopy. Biophys J 101:1539–1545
22. Scarcelli G, Polacheck WJ, Nia HT, Patel K, Grodzinsky AJ, Kamm RD, Yun SH (2015) Noncontact three-dimensional mapping of intracellular hydromechanical properties by Brillouin microscopy. Nat Methods 12:1132

23. Schreiber E, Anderson O, Soga N (1973) Elastic constants and their measurement. McGraw-Hill, Ann Arbor
24. Koski KJ, Akhenblit P, McKiernan K, Yarger JL (2013) Non-invasive determination of the complete elastic moduli of spider silks. Nat Mater 12:262–267
25. Palombo F, Winlove CP, Edginton RS, Green E, Stone N, Caponi S, Madami M, and Fioretto D (2014) Biomechanics of fibrous proteins of the extracellular matrix studied by Brillouin scattering. J R Soc Interface 11
26. Duck F (1990) Physical properties of tissue. Academic Press, London
27. Fabry B, Maksym GN, Butler JP, Glogauer M, Navajas D, Fredberg JJ (2001) Scaling the microrheology of living cells. Phys Rev Lett 87:1481021–1481024
28. Dil JG (1982) Brillouin-scattering in condensed matter. Rep Prog Phys 45:285–334
29. Sandercock JR (1975) Some recent developments in Brillouin scattering. Rca Review 36:89–107
30. Randall J, Vaughan JM (1982) The measurement and interpretation of Brillouin scattering in the lens of the eye. Proc R Soc London Ser B 214: 449–470
31. Vaughan JM, Randall JT (1980) Brillouin scattering, density and elastic properties of the lens and cornea of the eye. Nature 284:489–491
32. Scarcelli G, Yun SH (2008) Confocal Brillouin microscopy for three-dimensional mechanical imaging. Nat Photonics 2:39–43
33. Shirasaki M (1996) Large angular dispersion by a virtually imaged phased array and its application to a wavelength demultiplexer. Opt Lett 21:366–368
34. Scarcelli G, Kim P, Yun SH (2008) Cross-axis cascading of spectral dispersion. Opt Lett 33:2979–2981
35. Scarcelli G, Yun S (2011) Multistage VIPA etalons for high-extinction parallel Brillouin spectroscopy. Opt Express 19:10913–10922
36. Berghaus K, Zhang J, Yun SH, Scarcelli G (2015) High-finesse sub-GHz-resolution spectrometer employing VIPA etalons of different dispersion. Opt Lett 40:4436–4439
37. Berghaus KV, Yun SH, Scarcelli G (2015) High speed sub-GHz spectrometer for Brillouin scattering analysis. J Vis Exp 106:53468
38. Zhang J, Nou X, Kim H, Scarcelli G (2017) Brillouin flow cytometry for label-free mechanical phenotyping of the nucleus. Lab Chip 17(4):663–670
39. Fiore A, Zhang J, Shao P, Yun S, Scarcelli G (2016) High-extinction virtually imaged phased array-based Brillouin spectroscopy of turbid biological media. Appl Phys Lett 108:203701
40. Meng Z, Traverso A, Yakovlev V (2014) Background clean-up in Brillouin microspectroscopy of scattering medium. Opt Express 22:5410–5415
41. Remer I, Bilenca A (2016) Background-free Brillouin spectroscopy in scattering media at 780 nm via stimulated Brillouin scattering. Opt Lett 41:926–929
42. Shao P, Besner S, Zhang J, Scarcelli G, Yun S (2016) Etalon filters for Brillouin microscopy of highly scattering tissues. Opt Express 24:22232–22238
43. Antonacci G (2017) Dark-field Brillouin microscopy. Opt Lett 42:1432–1435
44. Antonacci G, Lepert G, Paterson C, Torok P (2015) Elastic suppression in Brillouin imaging by destructive interference. Appl Phys Lett 107:061102
45. Edrei E, Gather M, Scarcelli G (2017) Integration of spectral coronagraphy within VIPA-based spectrometers for high extinction Brillouin imaging. Opt Express 25:6895
46. Ballmann C, Thompson J, Traverso A, Meng Z, Scully M, Yakovlev V (2015) Stimulated Brillouin scattering microscopic imaging. Sci Rep 5:18139
47. Remer I, Bilenca A (2016) High-speed stimulated Brillouin scattering spectroscopy at 780 nm. APL Photonics 1:061301
48. Zhang J, Fiore A, Yun S, Kim H, Scarcelli G (2016) Line-scanning Brillouin microscopy for rapid noninvasive mechanical imaging. Sci Rep 6:35398
49. Besner S, Scarcelli G, Pineda R, Yun S-H (2016) In vivo Brillouin analysis of the aging crystalline lens. Invest Ophthalmol Vis Sci 57:5093–5100
50. Meng Z, Traverso A, Ballmann C, Troyanova-Wood M, Yakovlev V (2016) Seeing cells in a new light: a renaissance of Brillouin spectroscopy. Adv Opt Photon 8:300–327
51. Scarcelli G, Besner S, Pineda R, Kalout P, Yun SH (2015) In vivo biomechanical mapping of normal and keratoconus corneas. JAMA Ophthalmol 133:480–482
52. Scarcelli G, Kling S, Quijano E, Pineda R, Marcos S, Yun S (2013) Brillouin microscopy of collagen crosslinking: noncontact depth-dependent analysis of corneal elastic modulus. Invest Ophthalmol Vis Sci 54:1418–1425
53. Scarcelli G, Pineda R, Yun S (2012) Brillouin optical microscopy for corneal biomechanics. Invest Ophthalmol Vis Sci 53:185–190
54. Steelman Z, Meng Z, Traverso A, Yakovlev V (2015) Brillouin spectroscopy as a new method of screening for increased CSF total protein during bacterial meningitis. J Biophotonics 8:408–414
55. Moeendarbary E, Valon L, Fritzsche M, Harris AR, Moulding DA, Thrasher AJ, Stride E, Mahadevan L, Charras GT (2013) The cytoplasm of living cells behaves as a poroelastic material. Nat Mater 12:253–261
56. Antonacci G, Braakman S (2016) Biomechanics of subcellular structures by non-invasive Brillouin microscopy. Sci Rep 6:37217
57. Elsayad K, Werner S, Gallemi M, Kong J, Guajardo E, Zhang L, Jaillais Y, Greb T, Belkhadir Y (2016) Mapping the subcellular mechanical properties of live cells in tissues with fluorescence emission-Brillouin imaging. Sci Signal 9:rs5
58. Meng Z, Lopez S, Meissner K, Yakovlev V (2016) Subcellular measurements of mechanical

and chemical properties using dual Raman-Brillouin microspectroscopy. J Biophotonics 9: 201–207
59. Paszek MJ, Zahir N, Johnson KR, Lakins JN, Rozenberg GI, Gefen A, Reinhart-King CA, Margulies SS, Dembo M, Boettiger D, Hammer DA, Weaver VM (2005) Tensional homeostasis and the malignant phenotype. Cancer Cell 8:241–254
60. Hanahan D, Weinberg RA (2000) The hallmarks of cancer. Cell 100:57–70
61. Kumar S, Weaver V (2009) Mechanics, malignancy, and metastasis: the force journey of a tumor cell. Cancer Metastasis Rev 28:113–127
62. Payne SL (2005) Lysyl oxidase regulates breast cancer cell migration and adhesion through a hydrogen peroxide-mediated mechanism. Cancer Res 65:11429–11436
63. Mouw J, Yui Y, Damiano L, Bainer R, Lakins J, Acerbi I, Ou G, Wijekoon A, Levental K, Gilbert P, Hwang E, Chen Y, Weaver V (2014) Tissue mechanics modulate microRNA-dependent PTEN expression to regulate malignant progression. Nat Med 20:360
64. Fasching P, Heusinger K, Loehberg C, Wenkel E, Lux M, Schrauder M, Koscheck T, Bautz W, Schulz-Wendtland R, Beckmann M, Bani M (2006) Influence of mammographic density on the diagnostic accuracy of tumor size assessment and association with breast cancer tumor characteristics. Eur J Radiol 60:398–404
65. Khaled W, Reichling S, Bruhns OT, Boese H, Baumann M, Monkman G, Egersdoerfer S, Klein D, Tunayar A, Freimuth H, Lorenz A, Pessavento A, Ermert H (2004) Palpation imaging using a haptic system for virtual reality applications in medicine. Stud Health Technol Inform 98:147–153
66. Pepin K, Ehman R, McGee K (2015) Magnetic resonance elastography (MRE) in cancer: technique, analysis, and applications. Prog Nucl Magn Reson Spectrosc 90-91:32–48
67. Parker K, Doyley M, Rubens D (2011) Imaging the elastic properties of tissue: the 20 year perspective. Phys Med Biol 56:R1–R29
68. Miroshnikova Y, Mouw J, Barnes J, Pickup M, Lakins J, Kim Y, Lobo K, Persson A, Reis G, McKnight T, Holland E, Phillips J, Weaver V (2016) Tissue mechanics promote IDH1-dependent HIF1 alpha-tenascin C feedback to regulate glioblastoma aggression. Nat Cell Biol 18:1336
69. Zaman MH, Trapani LM, Siemeski A, MacKellar D, Gong HY, Kamm RD, Wells A, Lauffenburger DA, Matsudaira P (2006) Migration of tumor cells in 3D matrices is governed by matrix stiffness along with cell-matrix adhesion and proteolysis. Proc Natl Acad Sci U S A 103:10889–10894
70. Corbin EA, Kong F, Lim CT, King WP, Bashir R (2015) Biophysical properties of human breast cancer cells measured using silicon MEMS resonators and atomic force microscopy. Lab Chip 15:839–847
71. Cross S, Jin Y-S, Tondre J, Wong R, Rao J, Gimzewski J (2008) AFM-based analysis of human metastatic cancer cells. Nanotechnology 19:384003
72. Hartono D, Liu Y, Tan PL, Then XYS, Yung L-YL, Lim K-M (2011) On-chip measurements of cell compressibility via acoustic radiation. Lab Chip 11: 4072–4080
73. Li Q, Lee G, Ong C, Lim C (2008) AFM indentation study of breast cancer cells. Biochem Biophys Res Commun 374:609–622
74. Nikkhah M, Strobl JS, Schmelz EM, Agah M (2011) Evaluation of the influence of growth medium composition on cell elasticity. J Biomech 44:762–766
75. Swaminathan V, Mythreye K, O'Brien ET, Berchuck A, Blobe GC, Superfine R (2011) Mechanical stiffness grades metastatic potential in patient tumor cells and in cancer cell lines. Cancer Res 71: 5075–5080
76. Guck J, Schinkinger S, Lincoln B, Wottawah F, Ebert S, Romeyke M, Lenz D, Erickson H, Ananthakrishnan R, Mitchell D, KÃs J, Ulvick S, Bilby C (2005) Optical deformability as an inherent cell marker for testing malignant transformation and metastatic competence. Biophys J 88:3689–3787
77. Baker EL, Lu J, Yu D, Bonnecaze RT, Zaman MH (2010) Cancer cell stiffness: integrated roles of three-dimensional matrix stiffness and transforming potential. Biophys J 99:2048–2057
78. Tilghman RW, Cowan CR, Mih JD, Koryakina Y, Gioeli D, Slack-Davis JK, Blackman BR, Tschumperlin DJ, Parsons JT (2012) Matrix rigidity regulates cancer cell growth and cellular phenotype. PLoS One 5:e12905
79. Weder G, Hendriks-Balk MC, Smajda R, Rimoldi D, Liley M, Heinzelmann H, Meister A, Mariotti A (2014) Increased plasticity of the stiffness of melanoma cells correlates with their acquisition of metastatic properties. Nanomed Nanotechnol Biol Med 10:141–148
80. Solon J, Levental I, Sengupta K, Georges PC, Janmey PA (2007) Fibroblast adaptation and stiffness matching to soft elastic substrates. Biophys J 93: 4453–4461
81. Nelson C, Bissell M (2006) Of extracellular matrix, scaffolds, and signaling: tissue architecture regulates development, homeostasis, and cancer. Annu Rev Cell Dev Biol 22:287–309
82. Yamada KM, Cukierman E (2007) Modeling tissue morphogenesis and cancer in 3D. Cell 130: 601–610